Light Intensity Profiles in a Perfectly Mixed Photoreactor

SOLOMON M. JACOB and JOSHUA S. DRANOFF

Northwestern University, Evanston, Illinois

The light intensity distribution in a perfectly mixed photoreactor has been studied experimentally and analytically. Experimental measurements of intensities within the reactor were made with a specially designed light probe. These data were then used to test the validity of a model which treats the ultraviolet lamp as a linear source radiating in all directions. It was found that this model, which seems appropriate and allows reasonable computations, is somewhat in error owing to the neglect of the finite size of the lamp and the existence of reflection and refraction effects within the reactor. An empirical correction function was determined for use with the model which then yields predictions in close agreement with experimental data when the reactor is filled with a light absorbing liquid.

One of the complicating aspects of photoreactor design is the existence of nonuniform reaction rates throughout any finite reaction volume, even in the absence of concentration gradients. Such variations in rate arise because of light intensity profiles due to radiation absorbed by reactant and product, as well as divergence of the light from its source. If accurate reactor design and scale-up are to be carried out, it is essential that light intensity profiles be known precisely throughout the reactor volume.

The objectives of this paper are to demonstrate an experimental technique for determining light intensity profiles in a common reactor configuration and to point out some difficulties in the formulation of predictive models for such profiles. The type of device in question is a cylindrical annular reactor with a light source mounted along its centerline. Such a reactor has found application in previous studies (*1* to *3*) and is of interest for both research and industrial purposes.

It should be noted that no previous attempts to determine true light intensity profiles within a photoreactor have been reported. Rather it has generally been assumed (*1, 2, 4* to *7*) that a tubular light source could be represented as a line source with all radiation emitted normal to the lamp axis, that is, along cylindrical radius vectors only. Although mathematically convenient, the assumption of radial light is clearly not physically realistic except perhaps at the midpoint of the lamp some distance from its axis. The present work will demonstrate the seriousness of such assumptions. Furthermore, the details of a semiempirical analysis which accounts for nonradial radiation, as well as reflection and refraction effects, will be presented. It will be shown that this analysis yields results which agree closely with experimental measurements and can be used effectively in the treatment of reactor performance data.

This work has drawn its principal impetus from previous studies of the perfectly mixed annular reactor in this laboratory. These studies (*1* to *3*) indicated the uses and failings of simplified treatments of light intensity profiles and paved the way for the more rigorous and detailed analysis presented here.

Solomon M. Jacob is with Mobil Oil Company, Paulsboro, New Jersey.

ANALYSIS

The reactor configuration of interest is illustrated in Figure 1. This device, which was used in earlier studies, has been described in detail previously (*2*). Suffice it to say here that the reactor is made of acrylic plastic with the exception of an inner Pyrex wall. It is equipped with a General Electric F8T5/BLB ultraviolet lamp which emits its radiation in a relatively narrow band centered around 3,500Å. [The spectral energy distribution of the lamp is given elsewhere (*2, 3, 8*).] Because of the design of the lamp holder, radiation is received within the reaction volume only from those points along the lamp which correspond to the 4-in. height of the reactor. As shown,

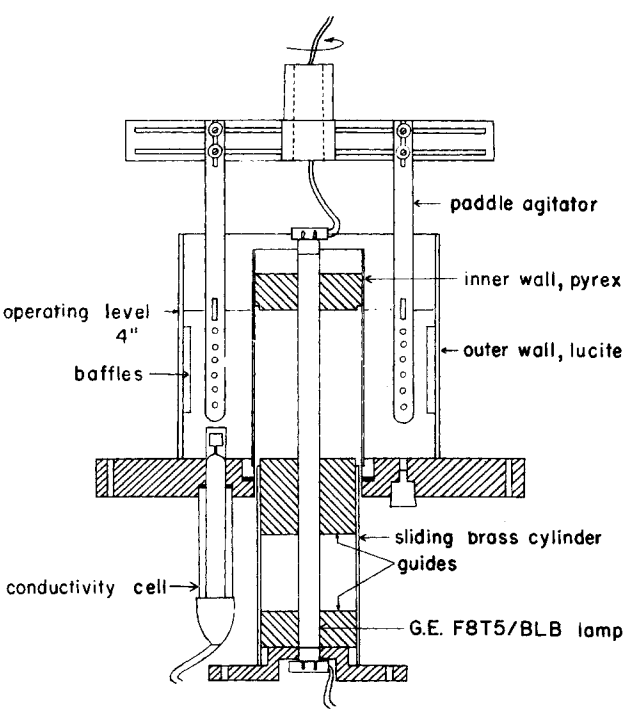

Fig. 1. Reactor configuration.

the reactor is equipped with a paddle stirrer to achieve the desired complete mixing of the liquid phase reaction volume.

The problem of interest is now to calculate the light intensity distribution within the reactor when it is filled with an attenuating medium of uniform composition. In order to carry out such calculations expeditiously, it is necessary to make some simplifying assumptions. The finite lamp is first approximated as a line source of the same length. The resultant intensity distribution within the attenuating solution is found by the well-known technique of integrating the equation for a point source over the length of the line. Since the integration cannot be handled analytically, it is replaced by a summation over a finite number of equivalent point sources distributed along the lamp length. The number of point sources is chosen large enough to minimize any errors in this approximation. The total intensity at any point in the reactor is then found by adding the contribution of each point source. Further simplification is achieved by neglecting refraction and reflection effects. The details of this approach follow.

Consider a volume element within the reactor with coordinates (r, z) as shown in Figure 2. From symmetry considerations, the angular functionality may be neglected. The intensity of light with wavelength λ at any point (r, z) within an attenuating medium due to a point source of strength $S_{p,\lambda}$ at a distance z' along the lamp is given by Lambert's law, corresponding to the following differential equation:

$$\frac{1}{\rho^2}\frac{d}{dp}(\rho^2 l_\lambda) = -\mu_{\lambda,c} l_\lambda \tag{1}$$

The spherical radius vector ρ is related to the cylindrical coordinates by

$$\rho^2 = r^2 + (z - z')^2 \tag{2}$$

Equation (1) may be integrated to yield

$$l_\lambda = \frac{S_{p,\lambda}}{4\pi\rho^2} e^{-(\mu_{\lambda,c})\rho} \tag{3}$$

Now, if the line source is to be represented by n such point sources, the strength of each point source will be related to the linear source strength per unit length $(S_{L,\lambda})$ as follows:

$$S_{p,\lambda} = S_{L,\lambda}\frac{L}{n} = S_{L,\lambda}\Delta Z' \tag{4}$$

Each of the n point sources is taken to be located at the center of the corresponding $\Delta Z'$ segment. Equation (3) may be further modified to account for the facts that there is no absorption of light by the central air gap and that the absorption coefficient of inner Pyrex wall is $\mu_{\lambda,g}$. By using similar triangles, the intensity due to a point source is then given by Equation (5):

$$l_\lambda = \frac{S_{L,\lambda}\Delta Z'}{4\pi\rho^2} e^{-[\mu_{\lambda,c}(r-r_1)+\mu_{\lambda,g}t']\rho/r} \tag{5}$$

Finally, the total intensity at wavelength λ at a point (r, z) due to the entire line source may be found by summing Equation (5) over the source length:

$$I_\lambda(r, z) = \sum_{z'=L/2n}^{z'=L-L/2n} l_\lambda \tag{6}$$

This equation may be appropriately simplified in the absence of attenuation within the reactor and/or the inner wall. With no absorption at all, the line source intensity can be found explicitly. In this case, with the notation shown in Figure 3, the result is (9):

$$I_\lambda(r, z) = \frac{S_{L,\lambda}}{4\pi r}(\theta_1 + \theta_2) \tag{7}$$

This result was of value in determining the number of point sources required to give an accurate representation of the line source. The intensity profile calculated from Equation (7) was compared with that found by using the summation form of Equation (6) with no absorption. Numerical computations carried out on a digital computer showed that the error due to approximating the line source by ten equivalent point sources was about 0.1%. Hence, this level of approximation was used in all subsequent calculations.

Equation (6) represents the theoretical model for the light intensity profile within the cylindrical annular reactor containing an absorbing medium due to a central line source. It is idealized compared with a real case in which the source is finite in size and reflection and refraction effects within the reactor may be important. Since the possible magnitude of such effects was not at all clear, it was felt necessary to carry out experimental measurements

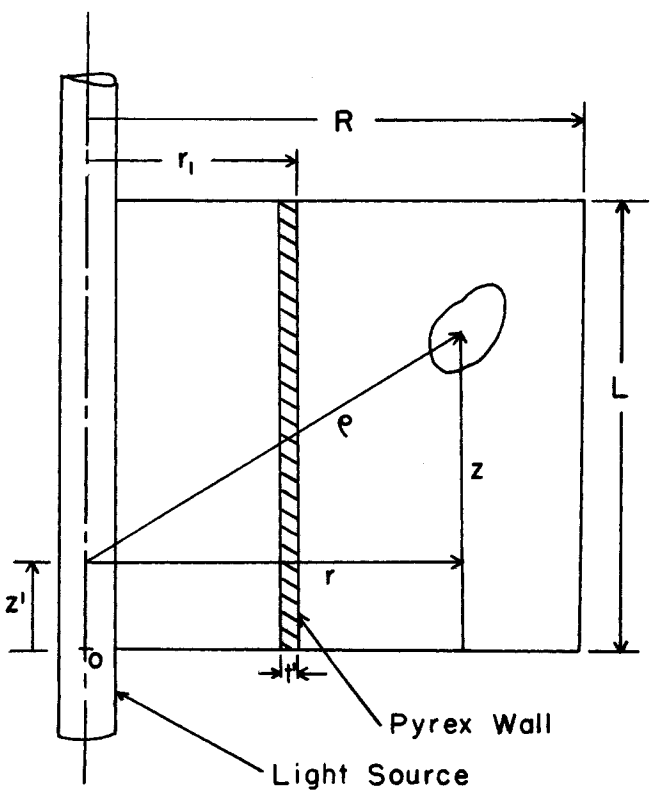

Fig. 2. Reactor geometry.

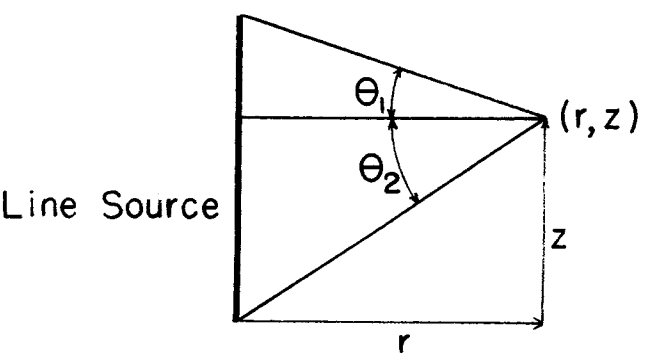

Fig. 3. Line source geometry.

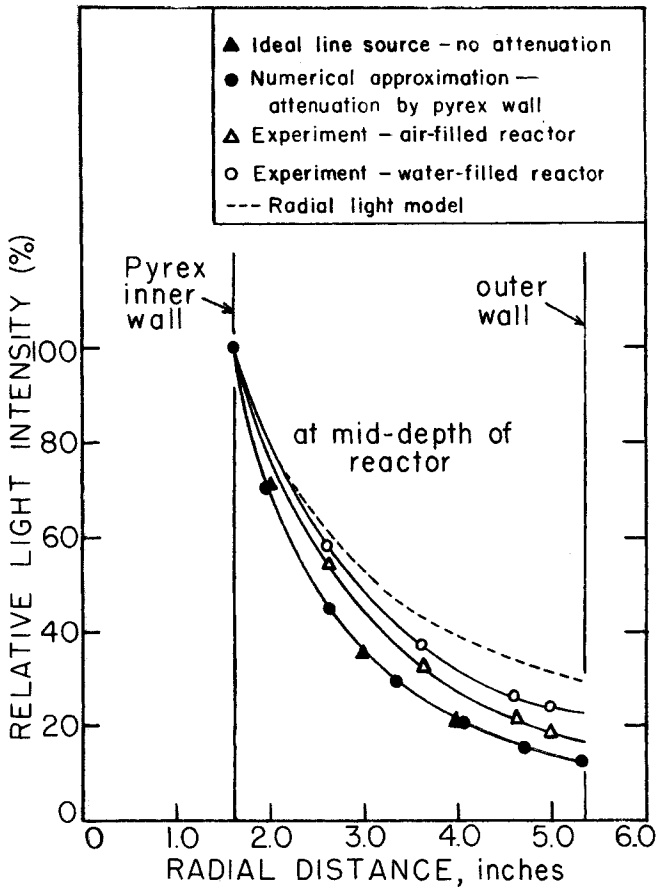

Fig. 4. Light intensity profiles.

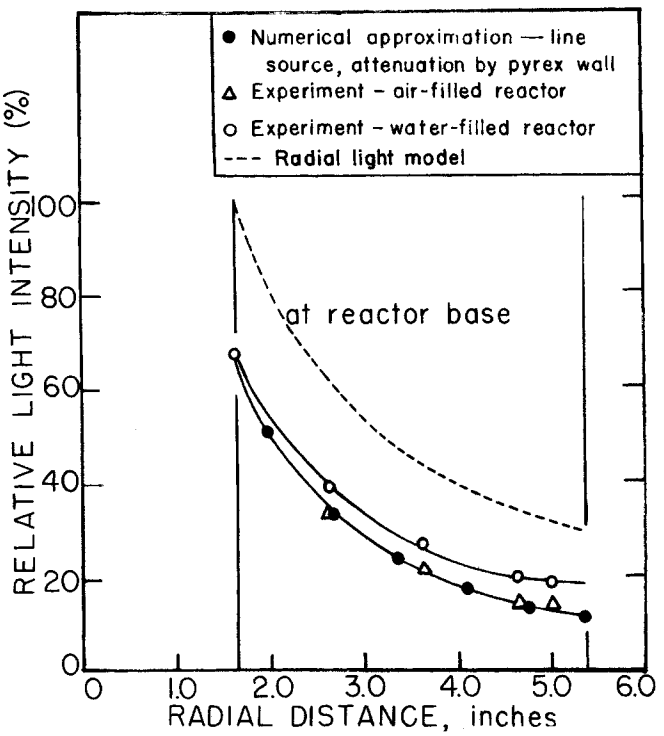

Fig. 5. Light intensity profiles.

of actual intensity distributions to test the adequacy of the ideal model and, if necessary, to determine an appropriate correction factor.

EXPERIMENTAL

A special light probe was designed and constructed to make the experimental intensity measurements. It consisted essentially of a selenium barrier photocell mounted on a glass tubing support and covered by a quartz window 1.4 mm. thick. The cell, which was ¼ in. in diameter, was attached to the quartz by epoxy cement, resulting in a probe with a light sensitive area ⅛ in. in diameter. The quartz window permitted the cell to receive radiation from points within a solid angle of approximately 120 deg., including all points on the lamp. This makes possible a true measure of intensity at any point. The photocell wires were run back through the tubing to a microammeter from which readings were obtained. The probe was attached to a support which permitted calibrated positioning within the reactor.

The actual photocell used was a commercially available type which responds to light in the wavelength range of interest. However, the response is not constant but rather varies uniformly from about 70% at 4,000 Å. to 30% at 3,000 Å. (*10*). This variation must be considered in the interpretation of experimental data. If light intensity is being measured under conditions of no attenuation or attenuation which is independent of wavelength, the current produced by the photocell will be directly proportional to light intensity. On the other hand, if wavelength dependent absorption of light is occurring, then the intensity distribution within the reactor will be different for each wavelength band. In this case, the photoprobe output will depend on the spectral sensitivity of the cell over wavelength bands and will, in fact, be just the sum of individual band intensities weighted by the appropriate response sensitivities. Note that intensity measurements in air and pure water correspond to the former case, while those made in reactant solution correspond to the latter situation.

In this work, the photocell output current was calibrated against a standard photometer and was found to be directly proportional to light intensity over the wavelength range of interest. Thus, current was taken to be a direct measure of intensity. Further experimental details are given elsewhere (*8*).

RESULTS AND DISCUSSION

Light intensity distributions were measured in the reactor when it was empty, filled with deionized water, and filled with a chloroplatinic acid reactant solution. The results and their interpretation follow.

Figure 4 shows data obtained with air and water for which no absorption occurs. These data were measured at the middepth of the reactor, that is, 2 in. from the top and bottom surfaces, and are all reported relative to the maximum light intensity within the reactor. This maximum occurs at middepth and at a radial distance of 1.615 in., which corresponds to the combined thickness of the central air gap, the Pyrex inner wall, and the quartz window of the photoprobe. Similar data measured near the reactor base are presented in Figure 5, again relative to the maximum intensity.

The lowest curve in Figure 4 compares calculated intensities based on the idealized line source, Equation (7), and the approximation by using Equation (6) with ten point sources and by accounting for absorption by the inner wall. These are in excellent agreement, confirming the validity of the approximation as well as the very slight effect of the Pyrex wall. The latter has good transmission characteristics for light of all wavelengths in the range of interest.

The figures also show measured intensities obtained in air and water. Clearly, these differ somewhat from the calculated values, especially at the reactor middepth. The deviations are undoubtedly due to the finite size of the source and the neglected effects of reflection and refraction. The finite source size produces more error as the source is approached more closely since the ideal intensity will tend to infinity as the distance decreases, while the actual in-

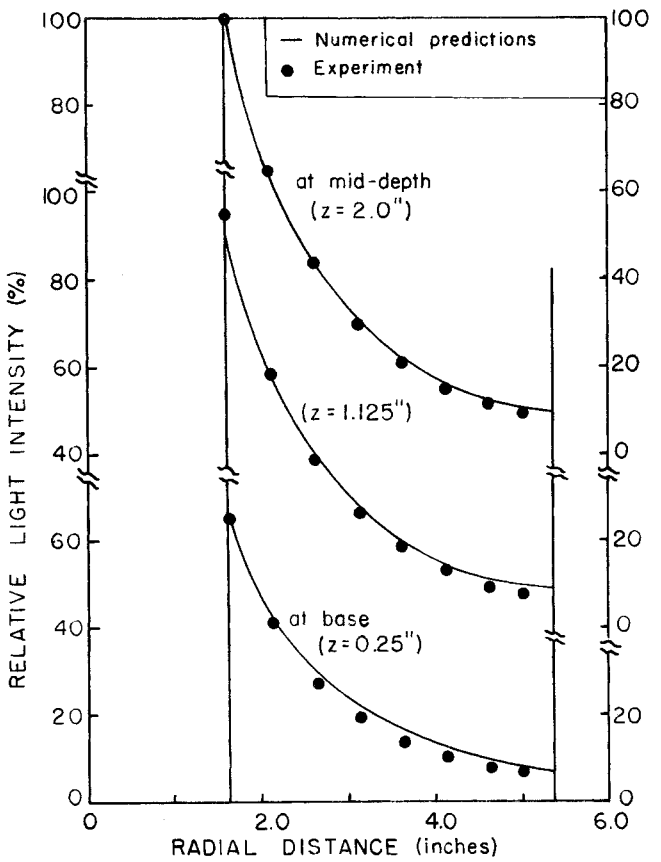

Fig. 6. Experimental vs. predicted profiles.

tensity must, of course, remain finite.

The reflection and refraction effects are most significant when water is present and especially at the middepth of the reactor. These act to make the intensity actually higher than predicted. In particular, refraction causes light rays which might otherwise leave the reactor at either end to be bent inward, thus concentrating the light. These effects should both be less important for reactors of larger length to width ratio.

For comparison, curves are also shown in Figures 4 and 5 for the radial or normal light model. Clearly, this model predicts intensities which are higher than the actual values and, of course, show no variation with depth.

Although the calculated and experimental intensities are all of the same order of magnitude, the differences at increasing radius are very significant in reactor performance calculations. Since reactor volume increases with the square of the radius, the outer regions of the annulus contribute heavily to the overall conversion in the vessel. Small differences in light intensities in these regions can have large effects on predicted performance. For this reason, it is very important that intensity distributions be known as accurately as possible.

Analysis of the experimental data for water and the calculated intensities at several reactor depths has led to the determination of an empirical factor by which the predicted values may be corrected to agree with the actual results within 2%. The form of this correction factor is shown in Equation (8):

$$C(r, z) = 1.0 + (r - 1.615)(0.13 + 0.0315z) \quad (8)$$

The utility of the correction factor may be tested by applying it to the prediction of light intensities when the reactor is filled with an absorbing liquid having an index of refraction near that of water. This restriction is necessary so that the reflection and refraction effects remain of the same order as those upon which $C(r, z)$ is based. Measurements were made, therefore, with the reactor filled with a solution 10^{-4} molar chloroplatinic acid having a conductivity of 9.0×10^{-5} mhos. This solution has been studied extensively in related investigations (*1* to *4*, *8*), and its transmission characteristics are known. In particular, the absorption coefficient is a known function of wavelength.

The true light intensity distribution for this solution should be predicted by applying Equation (6) to narrow wavelength bands and multiplying the results by the correction factor of Equation (8). Before comparison with experimentally measured intensities, these predictions must be further corrected for the spectral response sensitivity of the photoprobe as indicated earlier.

Figure 6 shows the resultant predicted values along with the actual experimental data for the lower half of the reactor. From these results, it is quite apparent that the corrected intensity profiles are in very close agreement with the data, and the validity of this approach is clearly demonstrated.

Because of the physical symmetry of the reactor, one might expect the intensity distribution to be symmetrical about the middepth as well. This is borne out by measurements, except very near the upper air-liquid interface. The reflective behavior of this surface should be different from the lower plastic surface. In addition, when the reactor is in operation, this surface will be disturbed by agitation. A more detailed analysis on that region has not been attempted at this point. It should be noted, however, that the assumption of symmetry seems quite satisfactory in actual reactor analysis (*3*).

No attempt was made in this study to predict the correction factor of Equation (8) or, equivalently, to calculate the profile in greater detail. Such a process would involve very cumbersome calculations in which the light source would be represented by a collection of point sources distributed over the curved lamp surface and in which every light ray would be allowed to undergo appropriate reflections and refractions. It was felt that such computations would be overwhelming in their numerical complexity and less useful than direct measurements.

CONCLUSION

This investigation has demonstrated a method for measuring the light intensity profiles within a photoreactor by using a special light probe. Comparison of these measurements with predictions of a simple line source model of the reactor lamp has shown the latter to be inadequate because of the neglect of reflection and refraction effects and the finite size of the actual lamp. However, it has been shown that a correction may be applied to yield a semiempirical model which is in excellent agreement with experimental data.

Although the specific results obtained here apply strictly to the reactor-liquid system studied, they illustrate effects which must be considered in analysis of light intensities within photoreactors and an approach which may be successfully applied to other systems.

ACKNOWLEDGMENT

The authors wish to express their sincere thanks to the National Science Foundation for its support of this work under grant GK-432.

NOTATION

l = light intensity, energy/area time
L = source length, length

n = number of point sources used to approximate the line source, dimensionless
r = cylindrical radial coordinate, length, in.
$S_{p,\lambda}$ = point source strength, energy/time
$S_{L,\lambda}$ = linear source strength, energy/length-time
t' = inner reactor wall thickness, length
z = reactor depth coordinate, length, in.
z' = linear source length coordinate, length

Greek Letters

λ = wavelength of radiation, length
ρ = spherical radial coordinate coordinate, length
θ = angle, radians
$\mu_{\lambda,c}$ = absorption coefficient for solution of concentration c, length^{-1}
$\mu_{\lambda,g}$ = absorption coefficient for Pyrex glass wall, length^{-1}

Subscript

λ = light of wavelength λ

LITERATURE CITED

1. Harris, P. R., and J. S. Dranoff, *AIChE J.*, **11**, 497 (1965).
2. Jacob, S. M., and J. S. Dranoff, *Chem. Eng. Progr. Symposium No. 68*, **62**, 47 (1966).
3. *Ibid., No. 89*, **64**, 54 (1968).
4. Dolan, W. J., C. A. Dimon and J. S. Dranoff, *AIChE. J.*, **11**, 1000 (1965).
5. Schechter, R. S., and E. H. Wissler, *Appl. Sci. Res.*, **A9**, 334 (1960).
6. Gaertner, R. F., and J. A. Kent, *Ind. Eng. Chem.*, **50**, 1223 (1958).
7. Huff, J. E., and C. A. Walker, *AIChE J.*, **8**, 193, (1962).
8. Jacob, S. M., Ph.D. dissertation, Northwestern Univ., Evanston, Ill. (1967).
9. Rockwell, T., "Reactor Shielding Manual," p. 392, Van Nostrand, Princeton, N. J. (1956).
10. "Solar Cell and Photocell Handbook," International Rectifier Corp., El Segundo, Calif. (1964).

Manuscript received January 26, 1968; revision received July 15, 1968; paper accepted September 11, 1968.

An Optimal Control Algorithm Using the Davidon-Fletcher-Powell Method with the Fibonacci Search

LOUIS G. BIRTA and PETER J. TRUSHEL

National Research Council, Ottawa, Ontario, Canada

A numerical method for solving a class of nonlinear optimal control problems is presented. The approach reformulates the associated two-point boundary value problem as a multidimensional minimization problem. This problem is, in turn, solved by using the method of Davidon-Fletcher-Powell. The one-dimensional minimization problem implicit in the implementation of the Davidon-Fletcher-Powell algorithm is handled with the Fibonacci search technique. Several examples are presented to demonstrate the effectiveness of the method for problems with and without magnitude constraints on the control variable(s).

A broad class of optimal control problems can, via the necessary conditions of the Pontriagin maximum (minimum) principle be recast as two-point boundary value problems. A variety of approaches to the solution of the boundary value problem have been suggested. One such approach (*1*) reformulates the boundary value problem as a multidimensional minimization problem. This is achieved by introducing an auxiliary error function whose minimization is equivalent to the solution of the boundary value problem. The intent of this paper is to demonstrate that the potential of this approach has not been fully exploited, especially in the light of recent advances in minimization techniques.

Among the first-order multidimensional minimization methods (those requiring only gradient information), a technique originally due to Davidon (*2*) and subsequently refined by Fletcher and Powell (*3*) has become widely accepted as one of the most powerful. It is demonstrated in this paper that the Davidon-Fletcher-Powell (henceforth DFP) algorithm can be effectively utilized in solving a wide class of optimal control problems by applying it to the auxiliary n dimensional minimization problem. A noteworthy property of the DFP algorithm is its capability of locating the minimum of a quadratic function of n variables, in at most n steps. In the context of the control algorithm suggested herein, this feature ensures that the linear system/quadratic cost problem can be solved in at most n iterations, where n is the dimension of the system state vector.*

The implementation of the DFP technique requires the solution of a one-dimensional minimization problem at each stage of the iterative process. In the proposed optimal control algorithm, the Fibonacci search technique is used to accomplish this task.

In many practical situations, the control variable(s) associated with the problem is (are) subject to magnitude constraints. It is shown via several examples that the solu-

* A formal proof of this appears in reference 4.